agriculture

MDPI

Article

DEM Study of Seed Motion Model-Hole-Wheel Variable Seed Metering Device for Wheat

Zhaodong Li [1,2], Jiyu Zhong [1], Xin Gu [1], Heng Zhang [1], Yongxin Chen [1,2], Weiwei Wang [1,2], Tian Zhang [1,2] and Liqing Chen [1,2,*]

[1] College of Engineering, Anhui Agricultural University, Hefei 230036, China
[2] Anhui Province Engineering Laboratory of Intelligent Agricultural Machinery and Equipment, Hefei 230036, China
* Correspondence: lqchen@ahau.edu.cn

Abstract: On the basis of the discrete element method (DEM), the movement of seed particles during the filling process of a wheat hole-wheel variable seed-metering device was numerically simulated. The impact of various model hole structures, filling postures, and vibration frequencies on the performance of filling was investigated. The results demonstrated that the average speed and filling posture of seeds varied significantly between models. The research demonstrated that the planter's filling effect was greatly enhanced by raising the average seed population speed in the confined region. Wheat seeds can be filled in the "flat" and "side" postures because the type of hole is conducive to smooth seed filling and the seed in the type of hole is not readily lost owing to vibration. The seed-metering devices adapt well to a vibrational environment, and the vibration factor has no discernible effect on the seed metering rate. The model holes (e.g., inverted fin-shaped holes) with the highest seed filling rate in the simulation test are employed in the bench test to validate the simulation model. The seed rate range was 300–3200 g/min, while the frequency of vibration was 0–10 Hz. Results indicated that the coefficient of variation of the stability of the total seeding rate was less than 1.3%, that the seeding rate of each row was consistent, and that the coefficient of variation was less than 3%, demonstrating that the simulation model was accurate and met the requirements of wheat agronomic seeding.

Keywords: DEM method; model; seed motion; wheat

check for updates

Citation: Li, Z.; Zhong, J.; Gu, X.; Zhang, H.; Chen, Y.; Wang, W.; Zhang, T.; Chen, L. DEM Study of Seed Motion Model-Hole-Wheel Variable Seed Metering Device for Wheat. *Agriculture* **2023**, *13*, 23. https://doi.org/10.3390/agriculture13010023

Academic Editor: Andreas Gronauer

Received: 19 November 2022
Revised: 11 December 2022
Accepted: 14 December 2022
Published: 21 December 2022

Copyright: © 2022 by the authors. Licensee MDPI, Basel, Switzerland. This article is an open access article distributed under the terms and conditions of the Creative Commons Attribution (CC BY) license (https://creativecommons.org/licenses/by/4.0/).

1. Introduction

Wheat is the most important food crop in China, and Jianghuai is one of the most important wheat-growing regions. The wheat business has progressively evolved from family farming to a pillar of agricultural and rural economic development [1]. The pace of mechanization of wheat planting is increasing daily. For many years, China has created wheat seed measuring equipment. However, there are not yet many seed meters that can plant varying quantities of wheat and are straightforward to use. This indicates that wheat planting efficiency must still be enhanced.

The hole-wheel model of seed-metering equipment has a straightforward design and can be utilized for a wide range of crops. According to a related study, Nibex Company manufactures a belt-type measuring system with a scoop-shaped seed-taking device. Boydas et al. [2] explored the effects of the vibration of the staggered seed feeding drum, the drum structure, and the amount of seed feeding on the uniformity of wheat seeding. Maleki et al. [3] created a seed metering device with a grain screw groove roller wheel. The speed of seed movement is effectively reduced by the screw grooved roller. The test results show that this type of hole wheel has a high seeding efficiency and reduces the phenomenon of flying seeds. Zagainov et al. [4] concentrated on developing strategies to eliminate seed misses in electrically powered single-seed metering devices and exploring the possibilities

of doing so. On the basis of varying the rotating speed of the seed metering drum, a novel method for avoiding seed misses in single-seed metering devices was introduced. Luo et al. [5] designed seed rows with four different types of holes and determined a ladybug-shaped hole through multiple sets of comparative tests, which effectively reduced seed damage. Zhao et al. [6] invented a kind of trin-type aspirating wheat seed platoon equipment and analyzed its seeding uniformity by comparing various types of suction hole structure in order to spread the seeds evenly. Pareek et al. [7] combined particle swarm optimization with an artificial neural network, a modeling method that can be used for the modeling and optimization of the seed chamber filling performance of a slant-plate seed arrangement device. Zhang et al. [8] designed a pneumatic cylinder-type precision seed arrangement device for direct seeding in Daodong and studied the influences of factors such as the type of skywheel structure, working speed, and vacuum degree of the suction chamber on the seed arrangement performance of the device. Zhang et al. [8] designed a pneumatic roller type precision seed arranger in order to solve the problem of high labor intensity in the current orderly broadcast production process of vegetables in the field, taking the qualification index, replay index, leakage index, and coefficient of variation of the seed arranger as evaluation indices. Li et al. [9] created a wheat precision seed feeder with a tilted parabolic hole to provide adequate wheat planting, improve seed supply efficiency, and ensure accurate seed supply. Panning et al. [10] created a mechanical seeding mechanism using various beet seeds, evaluated their seeding uniformity, and determined the influence of seeding speed and traveling speed on seed uniformity. Liu et al. [11] suggested that the problem of uneven seed distribution in wide-seedlings could be solved by combining the precision seed arrangement technology with a hook-shaped socket and a wheel-type precision seed arrangement device. This would result in more evenly distributed seeds in each row and less scattering of seeds between rows.

In seed metering device development, the discrete element method (DEM) is frequently employed. Based on the discrete element method, Gao et al. [12] report a numerical investigation of the movements of seed particles in a unique high-speed seed metering apparatus. Using a series of controlled numerical tests, the effects of important parameters such as the inlet velocity of particles, feeding rates, and the angle of the seed cleaning element are explored. Jin et al. [13] modified the opening of the fluted roller and the sowing clearance between the brush and the fluted roller of the seed metering device with the fluted roller, which is commonly used in wheat drill seeding, in order to increase work efficiency. Lai et al. [14] utilized EDEM software to assess the movement status of seeds in the filling area in order to address the issues of inadequate ginseng seed mobility, a high leakage rate, and a high seed damage rate during seed filling. Through analysis, the mechanism of the convex hull and special-shaped hole structure to increase the seed-filling performance of the seed metering device was clarified, and a wheel-type precision seed metering device with a convex hull and special-shaped holes was built. Lei et al. [15] investigated aspects of the seeding process that were not measurable based on DEM simulation and conducted bench experiments to determine seed dispersal uniformity. Zhang et al. [16] developed a model of a spoon-belt potato seed metering system based on EDEM, simulated the entire process of seed metering, and identified the optimal sowing-related parameters for enhancing the device's seed filling performance. Widely used in the field of agricultural engineering, EDEM simulation software can mimic the movement conditions of seeds following interaction with a metering device and population [17]. Previous research has demonstrated that decreasing seed-to-seed interaction and increasing seed activity within a population are favorable to increasing the seed fill rate. The works [18,19] constructed a seed plate with a hole-type head using EDEM software. The hole-type head was utilized to agitate the population and support the seeds, enhancing the adsorption performance. Through the EDEM numerical model and performance tests, Shi et al. [20] concluded that increasing population disturbance can immediately reduce the internal friction resistance of seeds, and they chose the combination-hole-type of seed arrangement plate.

The above research shows that the model-hole-wheel seed arrangement device can provide mechanical variable seed adding, a simple structure, and good efficiency. In this paper, based on the variable seed arrangement mechanism principle, a wheel-type variable seed arrangement device with inverted-fin-shape model hole structure was designed. Based on EDEM simulation, four common model holes were taken as the research object, and numerical simulation analysis was carried out. Through the simulation study, the structural reliability of various model holes and main components of the seeding system was verified. Through the analysis of the motion parameters of the filling chamber, the reasons for the high filling efficiency of the seeding system were discussed. A method was proposed for evaluating the seed filling performance of a hole-wheel seed metering device for wheat. The primary and secondary effects of rotating speed, model hole capacity opening, and vibration frequency on the seed filling performance of the seed discharging device were studied.

2. Material and Methods

2.1. Seed Metering Device Structure

The proposed inverted-fin-shaped hole-wheel variable seed metering system for wheat consisted primarily of a seed box, a seeding shell, a seeding shaft, a variable seeding mechanism, a seed cleaning brush, and a seed guiding tube, as depicted in Figure 1.

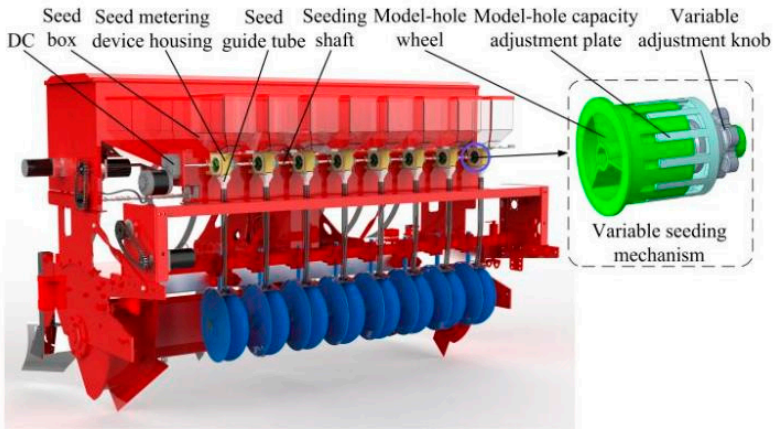

Figure 1. Mechanical variable direct seeder for wheat.

The variable seeding mechanism included a model-hole wheel, a model-hole capacity adjustment plate, and an adjustment knob. The model-hole wheel was installed in the rotating circular grooves on both sides of the seeding shell. The spokes of the model-hole capacity adjustment plate were matched with the long grooves of the model-hole wheel, and the model-hole volume can be changed from the adjustment knob. According to the topographical characteristics and the actual agronomic requirements of wheat sowing operations, the main technical parameters of the inverted-fin shaped model-hole wheel variable seed metering device for wheat are shown in Table 1.

Table 1. The main technical parameters of inverted-fin-shape model-hole-wheel variable seed metering device for wheat.

Parameter	Numerical Value
Length × width × height mm × mm × mm	368.5 × 180 × 460
Rotational speed of seed metering device r/min	20~110
Model hole capacity adjustment range mm	0~30
Operating speed km/h	3~7
Coefficient of variation of total seeding rate stability %	≤3.9
Coefficient of variation of each row seeding rate consistency %	≤1.3
Relative deviation between theoretical value and test value %	≤5.0
Rows	8~14 (Optional)

2.2. Working Principle of Seed Metering Device

The seeds fall to the upper seed-filling region of the seed metering mechanism and fill the model hole due to their own gravity. The seeds were limited by the inverted-fin-shaped model-hole structure and lateral pressure of the seed population in the seed filling chamber, and with the rotation of the hole-wheel model, the seeds went to the seed-clearing region. The seed cleaning brush is able to remove any seeds that were outside of the model's hole. The process of short-distance seeding is completed when the model hole spins to the lower seed-delivering location and falls out of the model hole due to its own gravity. Figure 2 depicts the structure of the seed metering apparatus.

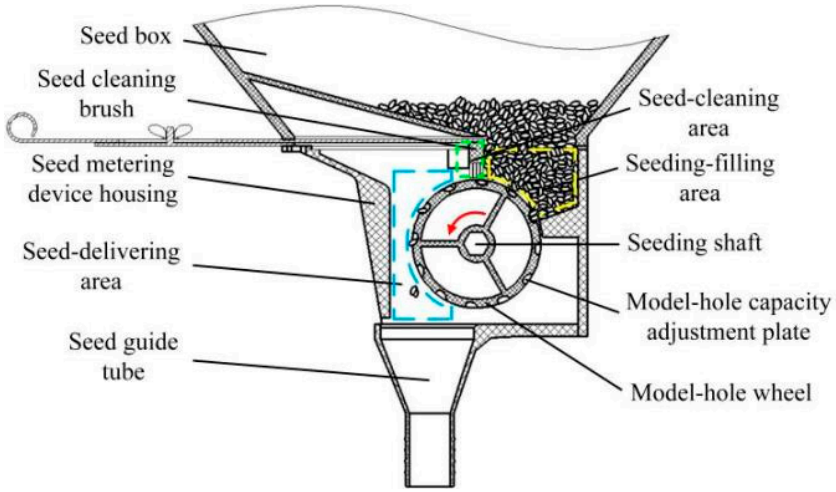

Figure 2. Seed metering device for wheat.

2.3. Seed Filling Posture in Model Hole

Wheat seeds are elliptical in shape and possess poor fluidity. They assume three positions during filling: "flat", "lateral", and "erect". Figure 3 depicts the filling position. The width and depth of the inverted-fin-shaped model-hole investigated in this work were 7 mm and 3 mm, respectively. In order to clarify the picking situation of seeds when filling seeds with shaped model-holes, this topic investigated the probability of different filling postures when filling wheat seeds and determined the influence of different types of model-holes on the different filling probabilities of seeds through simulation experiments, so as to confirm that inverted-fin model-holes were advantageous for seed filling in order to improve filling efficiency.

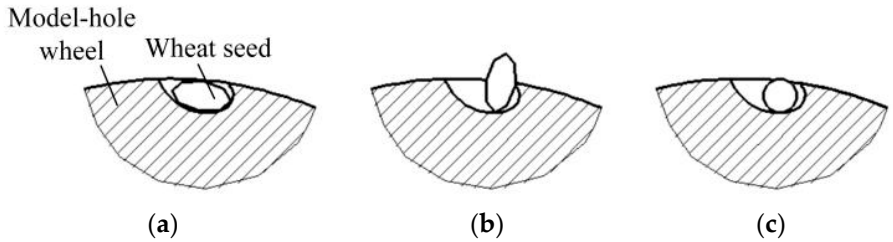

Figure 3. Three filling positions of wheat seeds. (**a**) "Flat"; (**b**) "Lateral"; (**c**) "Erect".

Through theoretical analysis, the occurrence probability of different filling postures of the wheat seed filling model-hole is proportional to the cross-sectional area of the seed:

$$\begin{cases} \frac{N_P}{N_S} = \frac{S_P}{S_S} \\ \frac{N_P}{N_C} = \frac{S_P}{S_C} \\ \frac{N_S}{N_C} = \frac{S_S}{S_C} \end{cases} \quad (1)$$

where N_P is the probability of the "flat" posture of seed, %; N_C is the probability of the "lateral" posture of seed, %; N_S is the probability of the "erect" posture of seed, %; S_P is the cross-sectional area of the "flat" posture of seed, mm^2; S_C is the cross-sectional area of the "lateral" posture of seed, mm^2; S_L is the cross-sectional area of the "erect" posture of seed, mm^2.

The filling posture of the seed filling the model-hole was an independent event, and the sum of probabilities was:

$$N_P + N_C + N_S = 100\% \tag{2}$$

Combining Equations (1) and (2) can get:

$$\begin{cases} N_P = \frac{S_P}{S_P+S_C+S_S} \times 100\% \\ N_C = \frac{S_C N_P}{S_P} \times 100\% \\ N_L = \frac{S_S N_P}{S_P} \times 100\% \end{cases} \tag{3}$$

Through theoretical analysis, the occurrence probability of different filling postures of the wheat seed filling model-hole was proportional to the cross-sectional area of the seed:

$$\begin{cases} S_P = \frac{\pi}{4} lw \\ S_C = \frac{\pi}{4} lt \\ S_S = \frac{\pi}{4} wt \end{cases} \tag{4}$$

where l was the length of wheat seed, mm; w was the width of wheat seed, mm; t was the thickness of wheat seed, mm.

The seeds were required to be filled into the model-hole in a variety of filling positions and continue to travel with the hole-wheel model, with the model-hole influencing the filling performance. After theoretical calculation, the likelihood of "flat" and "lateral" germination of Xuke No. 1 wheat seeds was comparatively high; the sum of these probabilities was 81.31 percent, while the probability of "erect" germination was only 18.69 percent. The reason was that the mass of wheat seeds had a shape akin to an ellipse, with its center near to the center. In this investigation, it was determined that it was most efficient to fill model-holes in the "flat" and "lateral" locations with wheat seeds.

2.4. DEM Simulation

In order to explore whether the inverted-fin-shaped hole-wheel model seed metering device has advantages in the seed filling process, another three common hole-wheel model types on the market were listed for optimization, and corresponding research was carried out based on DEM simulation tools.

2.4.1. Model and Simulation Parameters

In order to investigate the effect of the hole-type model on the seed filling performance of a seed metering device, discrete element simulation analysis based on the varied cross-sectional forms of the model-holes designed in the second chapter was performed in this article. As depicted in Figure 4, there were four distinct sorts of model-holes for X-direction meshing. They were inverted-fin-shaped, parabolic, bowl-shaped, and prismatic model holes.

In accordance with the seed box, seed meter housing, and seed cleaning brush described previously, the matching simulation model was built and assembled using the model-hole-wheel. Simultaneously, the structure of the seed box and the seed metering shell were validated for their rationality during the simulation procedure. In order to increase the spinning speed of EDEM, the overall model of the seed metering device was simplified during simulation. According to the degree of influence on the seed metering performance of the seed metering device, the model was reduced to the seed box, the seed

cleaning brush, the seed metering shell, and the kind of model-hole-wheel and wheat seed, as illustrated in Figure 5.

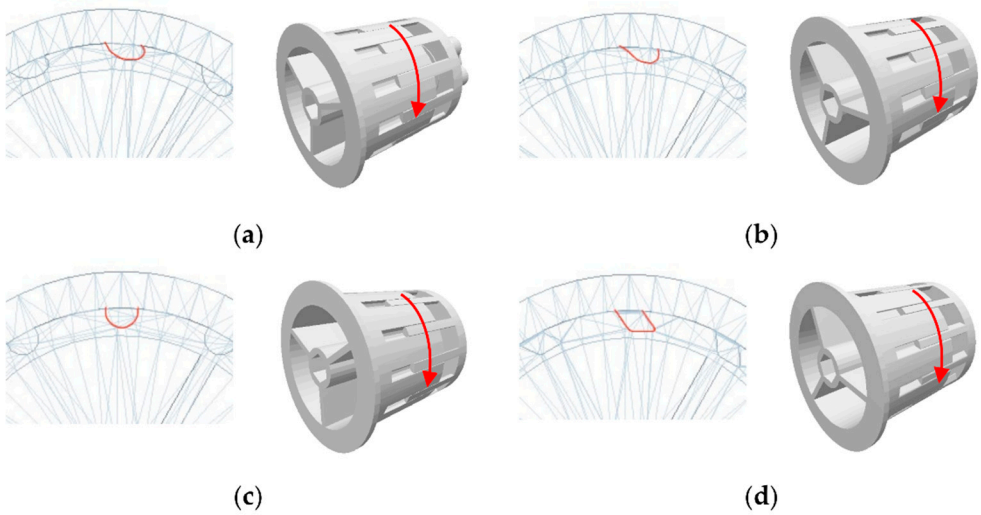

Figure 4. Four types of model-hole-wheels simulation models. (**a**) Inverted-fin-shape model-hole; (**b**) Inclined parabolic model-hole; (**c**) Bowl-shaped model-hole; (**d**) Prism-shaped model-hole; The curve of the shaped hole is represented by the red arrow.

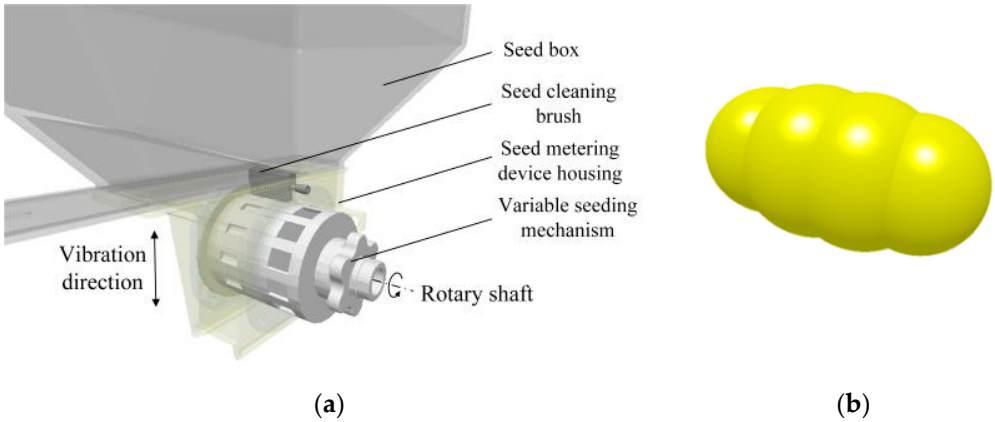

Figure 5. Simulation model. (**a**) Seed metering device model; (**b**) Wheat seed model.

Due of the ellipsoidal shape of wheat seeds, this study utilized four overlapping hard sphere models in place of the wheat seed model. The diameters of the hard sphere models with large radius and small radius were 3.0 mm and 2.6 mm, respectively. Figure 5b displays the three-dimensional representations of wheat seeds. Wheat seeds had a rather smooth surface, therefore the Hertz–Mindlin non-slip contact model was employed in the simulation, and the seed metering shell was manufactured using 3D printing technology. The model-hole-wheel was made of ABS plastic, as was the material utilized. According to the relevant literature [21], Tables 2 and 3 detail the material qualities of wheat seeds and ABS plastic, as well as the mechanical properties parameters between them.

Table 2. Physical properties of wheat and seed shells.

Project	Poisson's Ratio	Shear Modulus Pa	Density kg/m^3
Wheat	0.25	1.1 × 107	707.10
Seed housing/model-hole-wheel	0.30	2.7 × 1010	2700.00

Table 3. Collision coefficients between wheat and seeding shells.

Seed	Project	Crash Recovery Factor	Static Friction Coefficient	Coefficient of Kinetic Friction
Wheat	With wheat	0.44	0.50	0.01
	With seed housing/model-hole-wheel	0.44	0.30	0.01

2.4.2. Vibration Parameter Determination

Due to the concern that the vibration generated by external excitation may affect the normal operation of the seed metering device during field work of the inverted-fin-shaped model-hole-wheel-type wheat direct seeding machine, this topic collected vibration characteristic data of the machine during field operation. The vibration characteristics of the vibration test platform were calibrated using field-collected vibration data. The designed seed meter's metering capability was evaluated in a vibrational environment.

The vibration signal collection was carried out in Hanshan County, Maanshan, Anhui Province, from 10 to 12 December 2021. The test field was selected to be relatively flat and uncultivated land. The previous crop was rice, and the equipment was produced by Anhui Hongxiang Agricultural Machinery Co. Ltd. (Maanshan, China) The 2BQG-8 mechanical multi-function broadcast machine uses a CFF1004 wheeled tractor as the traction power. In order to obtain the field vibration parameters, please refer to the related literature [22,23]. In the time domain signal of the sensor's three axes, the time domain signal amplitude corresponding to the Z channel was much larger than that of the X channel and the Y channel. It can be seen that the field vibration was mainly in the vertical direction. Therefore, the Z channel of the PCB 356A32 three-axis acceleration sensor was used to collect the vibration signal in the vertical direction of the 2BQG-8 mechanical multi-function broadcast machine. During the test, the sensor was installed on the seed meter, and the field data collection situation was shown in Figure 6.



Figure 6. Vibration test and sensor installation position of inverted-fin-shaped model-hole-wheel variable seed metering device for wheat.

The travel speed of the tractor was set to the second slowest setting, while the working speed of the seed meter was set to 40 r/min. In the test, the acceleration time domain signal was collected by Labview, the continuous sampling frequency was set to 2500 Hz, the vibration signal was collected for 15 s, and Matlab was used to process the signal to obtain the frequency domain signal of the relationship between the vibration frequency and the vibration acceleration, as depicted in Figure 7a.

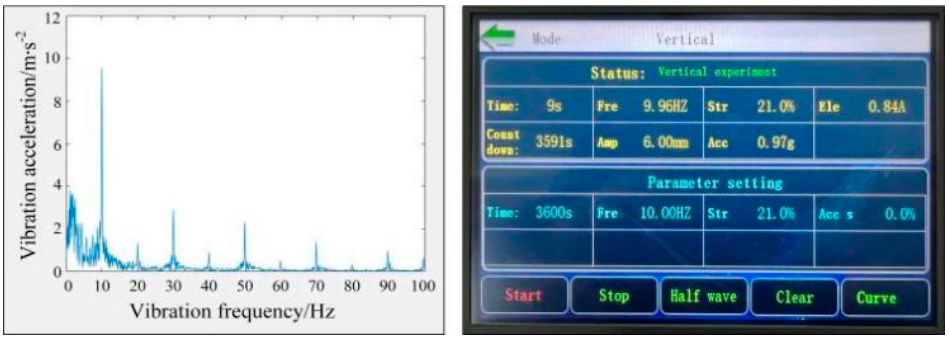

(**a**) (**b**)

Figure 7. Vibration frequency analysis and parameter setting. (**a**) Vibration frequency domain diagram; (**b**) Test bench parameter setting.

Figure 7a reveals that the predominant vibration frequency under these test conditions was 10 Hz. In other words, when the vibration frequency was 10 Hz, the highest acceleration was 9.60 m/s^2, which corresponds to 0.97 g. According to the analysis of the real test conditions, the field terrain, the vibration of the tractor engine, and the seeding motor affected the primary frequency of the vibration. In order to meet the field conditions, the disturbance between populations was increased, and the efficiency of seed filling was enhanced; the relationship between the vibration frequency of the actual field planter and the unilateral amplitude was determined, and the unilateral amplitude reached a maximum within the vibration frequency range of 0~10 Hz. As the frequency continued to climb, the acceleration of the vibration decreased. The maximum vibration frequency during this test's sampling interval was 10 Hz. According to the study, the vibration frequency of 0~10 Hz can be utilized to replicate the maximum acceleration during field vibration in order to validate the seed metering equipment. Adaptability set the vibration frequency parameter interval of the bench test to 0~10 Hz, taking three gradients of 0 Hz, 5 Hz, and 10 Hz, and set the vibration acceleration to 0.97 g. Figure 7b depicts the vibration test bench's parameter settings.

2.4.3. Experimental Design and Evaluation Methods

The numerical simulation test of the model-hole pattern utilizes the four model-hole patterns given in Chapter 3 as study items, and the period of each simulation was set to 10 s. Three gradients at 20, 30, and 40 r/min were chosen to calculate the rotational speed. For the model capacity, three gradients of 10, 15, and 20 mm were selected. The number of models needed to be sufficient to ensure that seeds remained in the seeding chamber of the seed metering device after a single simulation test, and it was difficult for an excessive number of models to slow down the device's operation. The particle control field's production pace was set to 50,000 seeds per second, and all 10,000 seeds were placed. Within 0.2 s, all seed models were formed, and the population close to the model-hole-wheel was in a static state. The seeding shaft was configured to rotate the model-hole-wheel every 0.2 s, and the simulation lasted 10.2 s. The fixed time step was 25% of the Rayleigh time step [24], and the simulation test was performed five times for each type of model-hole.

The seed population migration in the seed filling chamber can be used to reflect the seed filling effect of the hole-wheel [25]. In order to facilitate observation, after completion of the simulation, it will enter the Analyst post-processing module of EDEM. The clipping tool in EDEM was used to cut the simulation model along the surface of the seed disk, and the seed-filling chamber was divided into regions, dividing the results as shown in Figure 8. The size of the chamber will be determined by the speed of the seed population, which is divided into actual filling areas and dragged filling areas. The actual filling area is close to the model-hole-type wheel and close to the hole of the seed population area. The width of the area is slightly larger than the opening hole capacity. It continuously disturbs

the seed population depending on the depth of the pore structure. The drag filling area is the other area close to the hole-wheel-type, and the seed population in this area contacts the hole-wheel and is dragged along with its rotation. The seed population velocity in the actual filling area was large, and the seed population velocity gradually decreased with the distance from the type of hole-wheel. At this time, the seed population in the actual filling area could maintain a continuous relative motion with the rotation of the type of hole-wheel, and the disturbance effect could effectively improve the seed filling efficiency of the hole-wheel. The contact between the seed population and the hole-wheel in the drag filling area will produce friction force. The existence of this force makes the seed population always have a speed due to the relative motion with the hole-wheel, and the seeds far away from the hole-wheel in the filling chamber continuously replenish the hole. Because it has obtained some kinetic energy without filling the hole, it can minimize the relative velocity between the seed population and the wheel and further improve the filling efficiency. This study used the average speed of the seed population in the restricted area as an experimental index of the filling effect.

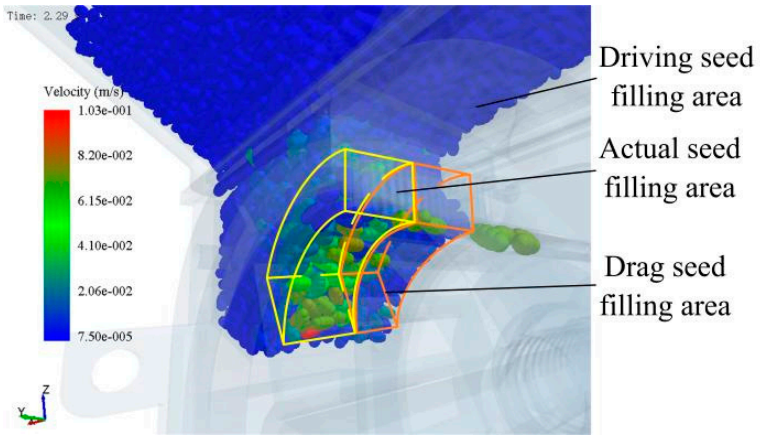

Figure 8. The division of the seed filling chamber of the seed metering device.

After the simulation, the EDEM post-processing Analyst tool was used to record the total number of seeds in a single test and the average number of seeds filled in a single model-hole, and to calculate the theoretical seed rate for a single test based on Equation (5). Multiple tests of the seed-metering device with the model-hole-wheel were conducted to determine the coefficient of variation of the stability of the seed-metering rate under varying vibration frequencies.

$$\begin{cases} m_{\mathrm{vk}} = \frac{6\bar{k}m_{\mathrm{k}}}{1000} \\ C_{\mathrm{V0}} = \frac{\sqrt{\frac{1}{u-1}\sum\left(k_{\mathrm{u}}-\bar{k}\right)^2}}{\bar{k}} \times 100\% \end{cases} \tag{5}$$

where m_{vk} is the seed metering rate of seed metering device under different vibration frequencies, mm; k is the average number of simulated particles under different vibration frequencies; m_{k} is 1000 seed mass, g; C_{V0} is the coefficient of variation of seed metering rate stability of seed metering device under different vibration frequencies, %; u is the number of tests with different vibration frequencies; k_{u} is the number of particles in a single simulation under different vibration frequencies.

2.5. Bench Test Plan

In order to verify the accuracy of the inverted-fin-shaped hole model, reflect on the benefits of the model-hole, and cite pertinent research, this paper designs four types of model-hole-wheels based on the characteristics of the model-hole structure, the function of picking up seeds in model-hole, and the objective of uniform seeding. The four sorts of

cross-sections were an inverted fin, an inclined parabola, a bowl, and a prism. This article utilized a 3D-printed ABS engineering plastics hole-wheel replica to ease the bench test.

Taking the four types of model-hole-wheels, the rotational speed, model-hole capacity opening, and evaluation index were the same as the measurement test of the influence degree of vibration frequency on the seed metering performance of the seed metering device. Four sets of seed metering devices were installed on the rack for optimum model-hole, and the construction of the test bench was shown in Figure 9.



Figure 9. Optimum test bench for model-hole type.

3. Result and Discussion

3.1. Simulation Model Verification

In order to study the seed filling performance of the inverted-fin-shaped model-hole-wheel seed metering device under different rotational speeds, model-hole capacity openings, and vibration frequencies, the other three common model-hole-wheel types on the market were listed, and the seeding rate was used as the evaluation. The bench test was carried out for the indicators, and the simulation test under the same conditions was carried out based on the DEM simulation tool, and the simulation value was compared with the experimental value to verify the accuracy of the simulation model. The results of the comparison are shown in Figure 10.

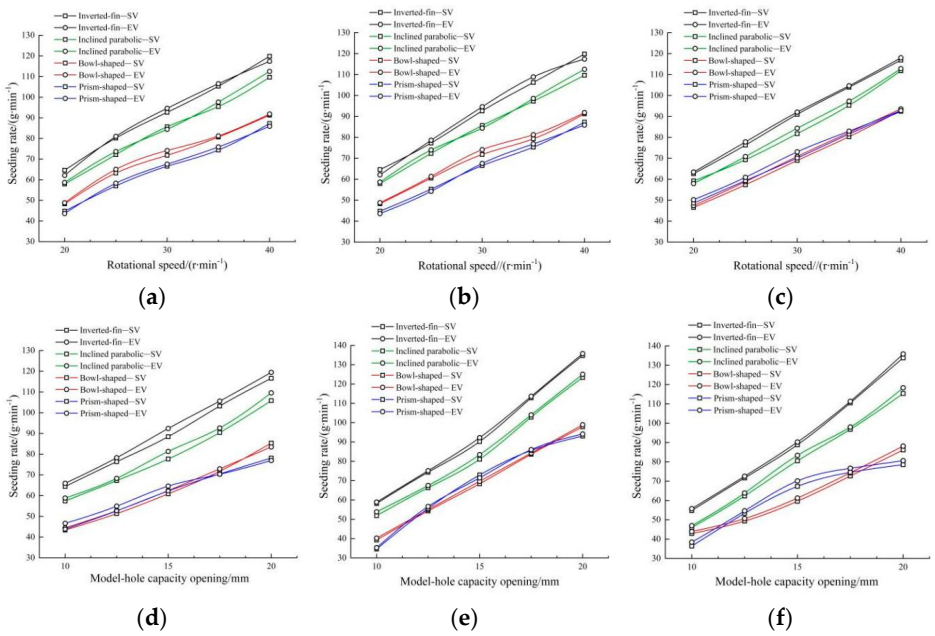

Figure 10. Comparison between simulation value and experimental value results. (**a**) Vibration frequency, 0 Hz; (**b**) Vibration frequency, 5 Hz; (**c**) Vibration frequency, 10 Hz; (**d**) Vibration frequency, 0 Hz; (**e**) Vibration frequency, 5 Hz; (**f**) Vibration frequency, 10 Hz.

Figure 10a–c showed the effects of different rotational speeds and vibration frequencies on the seeding rates of the four types of model-holes. Figure 8d–f showed the effects of different model-hole capacity openings and vibration frequencies on the seeding rates of the four types of model-holes. Through the bench test and simulation test comparison, we showed that the trend of the seeding rate curves of four types of model-holes was close under different rotational speeds, model-hole capacity openings, and vibration frequencies, indicating that the simulation model was accurate. In Figure 10, it can be clearly seen that the inverted-fin-shaped model-hole has a higher seeding rate and better seed filling efficiency. This model and the DEM simulation tool can be used to continue to study the reasons why the inverted-fin-shaped model-hole has better seed filling efficiency.

3.2. Analysis of the Numerical Simulation Test Result of the Model-Hole Pattern

Figure 11 illustrates each model-hole-wheel under the condition of the same vibration frequency. The number of seeds filled in the model-hole at a certain time was intercepted as a comparison. When the model-hole capacity opening of the wheat was set to 15 mm, it can be seen from Figure 11 that the number of wheat grains filled in a single model-hole of the inverted-fin-shaped model-hole-wheel reaches 4–5 grains, which is higher than the other three types of model-holes. It has the best seed filling effect, and there was no leakage and blocking phenomenon, effectively controlling the wheat broadcast demand. In summary, the multi-segment arc curve of the inverted-fin-shaped model-hole pattern was more conducive to filling seeds smoothly. The seeds in the model-hole were not easily lost due to vibration. Furthermore, the continuous migration of the seed population can be realized. Crops were used for both filling and seeding.

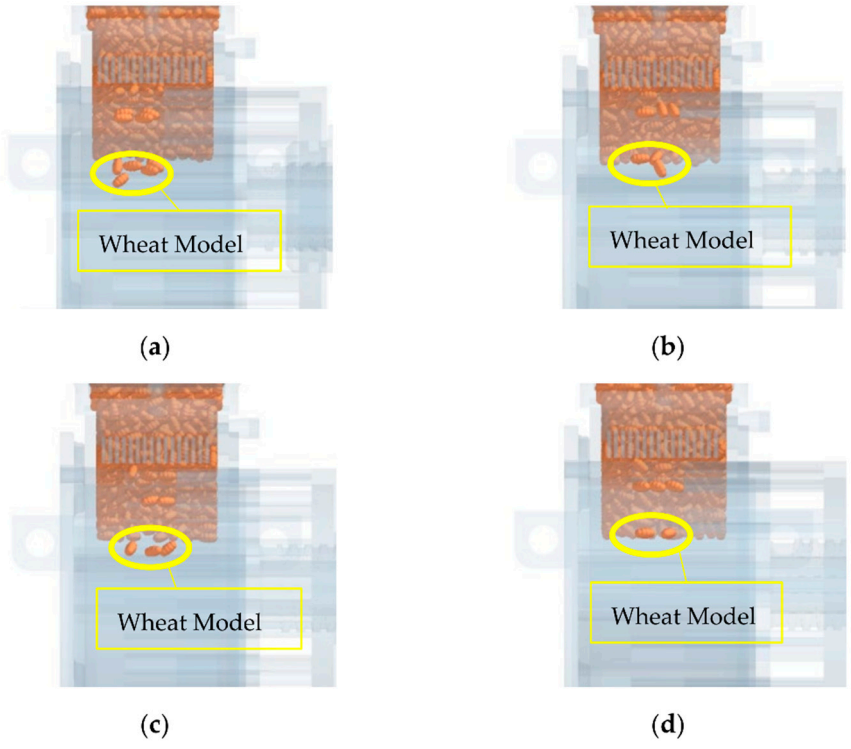

Figure 11. The number of grains of wheat seed filled with various model-hole types. (**a**) Inverted-fin-shape model-hole; (**b**) Inclined parabolic model-hole; (**c**) Bowl-shaped model-hole; (**d**) Prism-shaped model-hole.

Table 4 shows the results of the numerical simulation test of the model-hole type. The average number of grains of wheat in each type of model-hole-wheel was positively correlated with its rotational speed and the model-hole capacity opening and has a stable upward trend. According to the 1000-grain weight of the seeds, the seeding rate of the seed

metering device equipped with inverted-fin-shaped model-holes, inclined parabolic model-holes, bowl-shaped model-holes, and prismatic model-holes, respectively, was calculated. The rate was higher than the other three types of model-holes, and under different vibration frequencies, the rate of seeding did not change significantly. It showed that the inverted-fin-shaped model-hole type has higher seed filling efficiency, and the reasons for it were analyzed below.

Table 4. Numerical simulation results of seed filling performance of model-hole type.

Model-Hole Type	Working Rotational Speed r/min	Model-Hole Capacity Opening mm	Number of Particles in a Single Simulation			The Average Number of Seeds in Total	C_{V0} %
			Vibration Frequency 0 Hz	Vibration Frequency 5 Hz	Vibration Frequency 10 Hz		
Inverted-fin	20	10	175	165	170	170	2.94%
		15	267	255	249	257	3.57%
		20	398	395	418	404	3.10%
	30	10	258	242	242	247	3.73%
		15	353	346	335	345	2.63%
		20	594	569	573	579	2.32%
	40	10	323	305	300	309	3.91%
		15	475	460	441	459	3.71%
		20	760	716	749	742	3.09%
Inclined parabolic	20	10	162	132	142	145	10.51%
		15	255	249	232	245	4.86%
		20	375	389	372	379	2.40%
	30	10	236	189	196	207	12.25%
		15	339	326	308	324	4.80%
		20	539	548	493	527	5.60%
	40	10	276	283	260	273	4.32%
		15	460	441	416	439	5.03%
		20	690	730	674	698	4.13%
Bowl-shaped	20	10	90	116	120	109	14.99%
		15	204	188	175	189	7.69%
		20	295	301	269	288	5.90%
	30	10	185	200	185	190	4.56%
		15	278	262	245	262	6.31%
		20	432	435	361	409	10.23%
	40	10	235	279	252	255	8.69%
		15	407	380	368	385	5.19%
		20	545	548	490	528	6.19%
Prism-shaped	20	10	109	112	125	115	7.37%
		15	231	213	194	213	8.70%
		20	281	307	251	280	10.02%
	30	10	157	167	173	166	4.88%
		15	296	281	259	279	6.68%
		20	412	464	351	409	13.83%
	40	10	184	217	201	201	8.22%
		15	421	392	370	394	6.49%
		20	517	593	445	518	14.28%

Compared with the traditional rectangular columnar holes, the prismatic holes, designed based on the addition of two parallel planes with inclined angles, have better seed carrying efficiency. However, according to the optimization test of the prismatic holes, because the prismatic holes do not have an arc structure, they cannot fit well on the seed

surface, and the wheat seeds in the lateral-lying and upright state are easy to be cleared by the seed cleaning brush. The results were verified in the hole-type optimization experiment, and the prism-shaped hole and bowl-shaped hole openings were small, and the wheat seeds lying on the side and standing in the hole were easily squeezed by the parallel sections on both sides of the bowl hole, resulting in the "stuck seed" phenomenon. The seeds in the hole could not migrate to the seeding area and continued to migrate with the hole to the filling area, which hindered the filling of the seed chamber population. The seed filling efficiency is reduced, and the sowing amount is insufficient to meet the requirements of wheat sowing agronomy. The inverted-fin-type hole was significantly higher than the other three types of holes. In the simulation process of seed filling, the outer profile of wheat seed was always closely fitted with the large radius arc section at the end of the inverted-fin-shape hole section, and the seeds were difficult to fill in the upright position due to the extrusion action of the surrounding population, which significantly reduced the probability of seed clearing. The seed filling of rapeseed is intercut with the inverted-fin-shape hole contour, which is convenient for the population to fill the hole.

3.3. Seed Filling Attitude Analysis

From the above research, it can be seen that the number of seeds filled with inverted-fin-shaped model-holes was relatively stable. Figure 12 shows the wheat filling posture of different model-hole types at a certain time in the simulation. The wheat filling postures of inverted-fin and inclined parabolic model-holes were mostly "flat" and "lateral", bowl-shaped model-holes, and prism-shaped model-holes. A large number of model-holes appear in the "erect" posture of the seeds shown in the Figure 12.

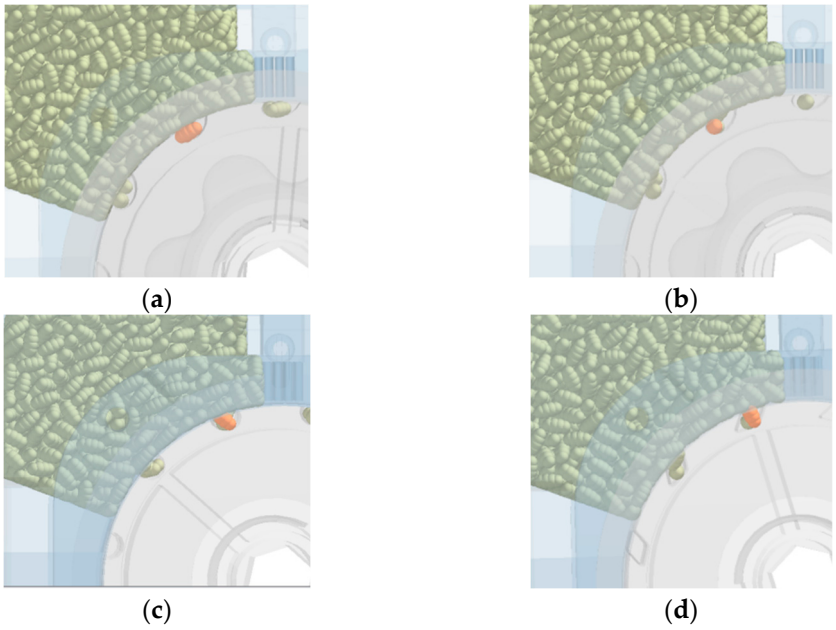

Figure 12. Seed filling posture. (**a**) Inverted-fin seed flat position; (**b**) Inverted-fin seed lateral position; (**c**) Bowl-shaped erect position; (**d**) Prism-shaped erect position.

When the population is moved to the clearing area in different postures, the seeds in the "flat" and "lateral" postures will not come into contact with the clearing brush, and they can pass through the clearing area smoothly. The seeds in the "erect" position were in too much contact with the seed cleaning brush and were easily removed from the model-hole by the seed cleaning brush, as shown in Figure 12. This affects how well the model-hole is filled with seeds and, in turn, the quality of the seeding.

The total number of wheat grains that appear in several different filling postures under each vibration frequency and rotational speed was counted. The results are shown in Table 5. Wheat seeds in the model-holes were mostly filled in the form of "flat" and

"lateral" in the inverted-fin-shaped model-holes was 82.18%, which was consistent with the above calculation results and was larger than that of the other three types. The outer contour of wheat seeds and the large-radius arc section at the end of the inverted-fin-shaped model-hole section always closely fit during the seed filling process, and the seeds were not easily filled in erect posture due to the extrusion of the surrounding population, which significantly reduces the probability of seeds being cleared and fully It showed that the design of the shaped model-hole is in line with the filling law and increases the efficiency of filling seeds.

Table 5. Different filling postures of wheat.

Model-Hole Type	T	T1	T2	T3	T1 + T2/%
Inverted-fin	3181	1342	1272	567	82.18
Inclined parabolic	3026	1210	1241	575	81.00
Bowl-shaped	2507	981	972	554	77.90
Prism-shaped	2657	1123	1060	474	82.16

Note: T: total number of seed particles, T1: stands for seeds "flat" number of attitude particles, T2: seeds "lateral" number of attitude particles, T3: seeds "erect" number of attitude particles.

3.4. Analysis of Population Migration Characteristics in Seed Filling Room

The seed filling room was divided into the actual seed filling area, the drag seed filling area, and the driving area, according to the population speed. The actual seed filling area was the population area that was close to the model-hole-wheel and close to the model-hole, and the width of this area was slightly larger than the volume opening of the model-hole. The drag seed filling area was other areas close to the model-hole-wheel, and the driving area was other areas in the seed filling room. The average speed of the population in the three regions was extracted, and the results are shown in Figure 13.

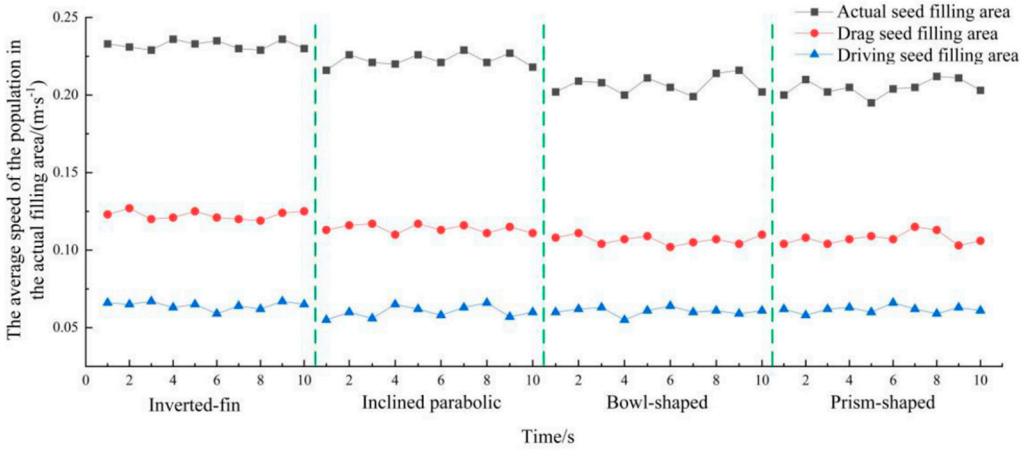

Figure 13. The average speed of the population in the three areas.

As shown in Figure 13, there were significant differences in the average velocity of the population in different filling areas with different model-hole types, and the higher average velocity was mainly concentrated in the actual filling area, which continuously perturbs the population depending on the depth of the structure; The drag average speed of the populations in the filling area was higher, and the populations were in contact with the model-hole-wheel and were dragged along with its rotation. In order to explore the reasons for the high seed filling efficiency of the inverted-fin-shaped model-hole type, the simulation results of each model-hole type under the conditions of vibration frequency of 10 Hz and rotational speed of 30 r/min were selected, and the four types of model-hole were used to analyze the filling process of seed filling through the Analyst tool. The migration speed of the population in the area was shown in Figure 14.

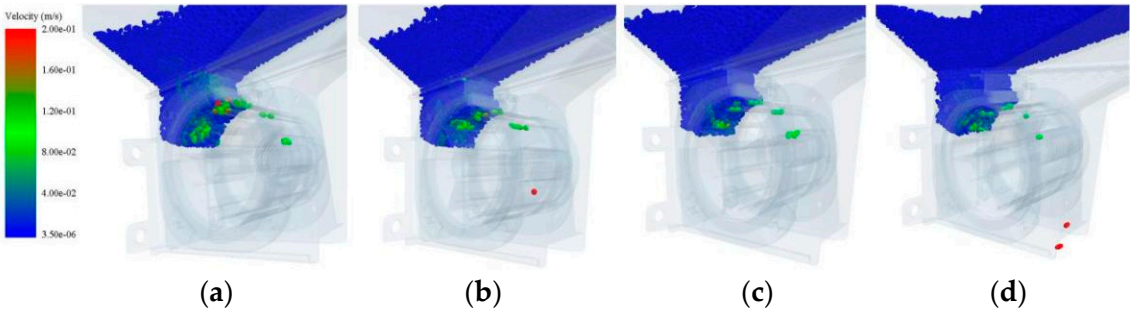

Figure 14. Migration speed comparison of wheat populations with different mod holes in same conditions. (**a**) Inverted-fin; (**b**) Inclined parabolic; (**c**) Bowl-shaped; (**d**) Prism-shaped.

It can be seen from Figure 14, that the actual seed filling area of the inverted-fin-shaped model-hole type has the largest volume and better continuity, and the average population migration speed was higher. The other three types of model-holes only had different speeds at the model-holes and were generally lower, and the dragging effect of dragging and filling the seed area was not significant. The Analyst tool was used to extract the population migration speed and the average number of seeds filled in the actual seed filling area. The extraction results are shown in Figures 15 and 16.

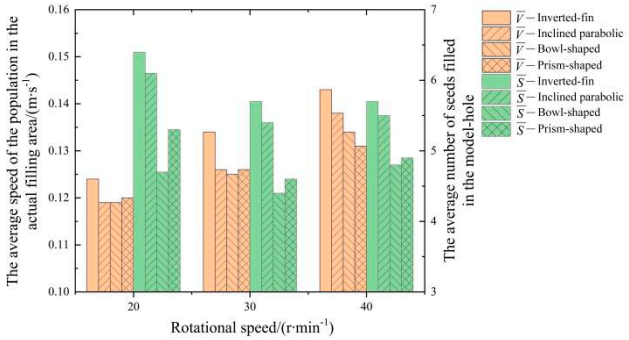

Figure 15. Effect of working speed on the average speed of the population and the average number of grains filled in the actual seed filling area of wheat.

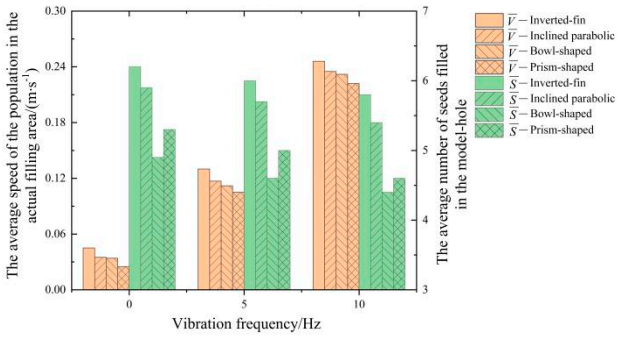

Figure 16. Effect of vibration frequency on the average speed of the population and the average number of grains filled in the actual seed filling area of wheat.

Figures 17 and 18 show the effects of the rotational speed and vibration frequency on the average speed of the population and the average number of seeds filled in model-holes in the actual wheat filling area. The results showed that with the increase of the rotational speed and vibration frequency, the actual filling average velocity of the population in the breeding area showed an increasing trend, and the inverted-fin-shaped model-hole was significantly higher than the other three types. The average number of seeds filled in each model hole was the highest when wheat was the research object. The number of species

was the most stable, and the vibration frequency had no significant effect on the filling process of the model-hole, and the adaptability was good. According to the above analysis, the average speed of the population in the actual seeding area with inverted-fin-shaped model-holes was the largest, the disturbance effect on the indoor population of seeding was the most significant, and the seeding effect was better. Looking back at the simulation results at a slow speed, it can be seen that when the small-radius arc at the front end of the inverted-fin-shaped model-hole runs, the velocity of the population in contact with it changes significantly, and this position was determined as the critical position. The inverted-fin-shaped model-hole was filled with seeds, but there was still some space, and the small radius arc of the model-hole can disturb the population in the actual seeding area and improve the population speed. Maintaining a continuous relative motion state, this disturbance effect can effectively improve the seed filling efficiency of the model-hole-wheel. The contact between the population and the model-hole-wheel in the dragging and filling area will generate frictional force. The existence of this force makes the population always move at a speed due to the relative movement with the model-hole-wheel. The filling model-hole was supplemented because it has obtained some kinetic energy when the model-hole was not filled, which can minimize the relative speed between the population and the model-hole-wheel and further improve the filling efficiency.

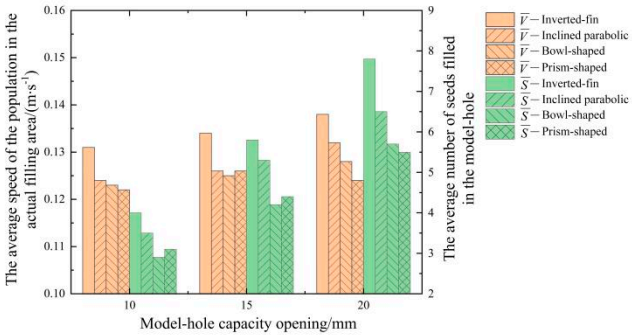

Figure 17. Effect of model-hole capacity opening on the average speed of the population and the average number of grains filled in the actual seed filling area.

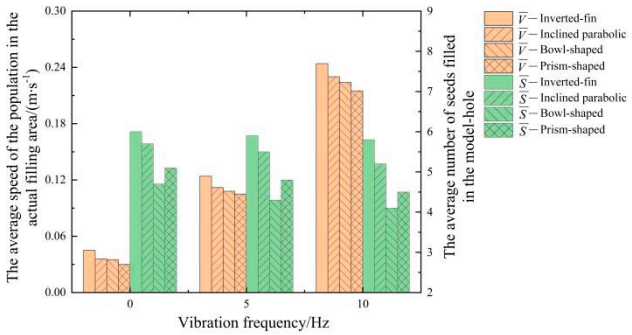

Figure 18. Effect of vibration frequency on the average speed of the population and the average number of grains filled in the actual seed filling area.

It can be seen from the figure that the primary and secondary order of the influencing factors affecting the seed filling performance of the seed metering device was the rotational speed > model-hole capacity opening > vibration frequency. The average number of seeds filled in the model-hole had a small difference, and the coefficient of variation was not more than 3%, indicating that the vibration frequency has no significant effect on the seed filling performance of the inverted-fin model-hole-type seed metering device.

3.5. Effect of Different Rotation Speed Range on Seeding Performance of Wheat

In order to improve the seeding performance of the inverted-fin-shaped model-hole-wheel-type variable seed metering device for wheat under different working conditions, this study selected Xuke No. 1 wheat seeds as the research object and investigated the seeding performance of the seed metering device under high-speed conditions. The test results are shown in Figure 19.

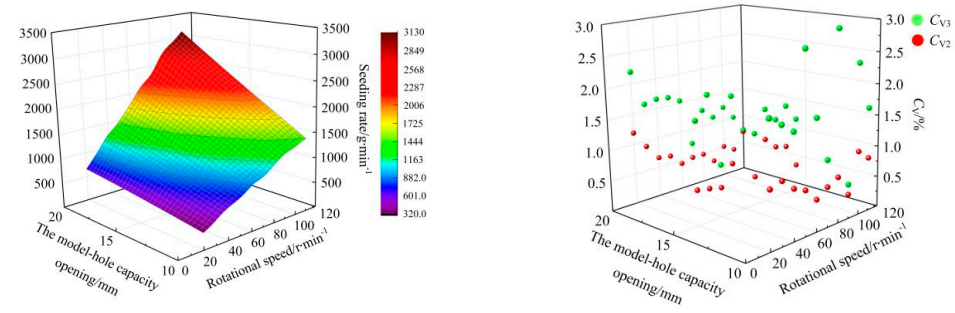

(**a**) (**b**)

Figure 19. Effect of different rotational speed and model-hole volume opening on wheat seed metering performance. (**a**) Seeding rate under different operating speed and model-hole capacity opening; (**b**) Seeding performance under different operating speeds and model-hole capacity opening.

Figure 19a shows the seeding rate of the seeding device under different rotational speeds and model-hole capacity openings. When the rotational speed was 20~110 r/min and the model-hole capacity opening was 10~20 mm, the seeding rate was 300~3200 g/min. As seen in Figure 19b, the coefficient of variation of the stability of the total seeding rate was not more than 1.3%, and the coefficient of variation of the consistency of the seeding rate in each row was not more than 3%, which is what agronomic technology requires.

The optimal fitting result was selected from it to obtain the theoretical value of the matching seeding rate under high-speed working conditions. According to the test data in Figure 19, the rotational speed was taken as the influencing factor. OriginPro was used to perform multiple linear regression analysis and unary linear regression analysis on the results of the experiment. The optimal fitting result was selected from it to obtain the theoretical value of the matching seeding rate under high-speed working conditions.

Based on multiple linear regression analysis, the model-hole capacity opening was increased as an additional evaluation index. The linear regression equation between the rotational speed and the model-hole capacity opening corresponding to the seeding rate was obtained by fitting:

$$m_v = 20.66n + 94.21L - 1314.34 \left(R^2 = 0.9363\right) \quad (6)$$

Based on unary linear regression analysis, one-variable linear fitting was performed on the capacity opening of different types of model-holes. The linear regression equation between the rotational speed and the seeding rate was obtained:

$$\begin{cases} m_{v10} = 12.99n + 75.86 & \left(R^2 = 0.9970\right) \\ m_{v15} = 20.57n + 115.91 & \left(R^2 = 0.9982\right) \\ m_{v20} = 28.42n + 92.64 & \left(R^2 = 0.9986\right) \end{cases} \quad (7)$$

where m_{vt} is the wheat seeding rate under different model-hole capacity openings, g/min, (t is 10, 15, 20, mm); n is the rotational speed of the model-hole-wheel.

It can be seen from the fitting results that the multivariate linear fitting results were not significant ($R^2 < 0.95$) with the rotational speed and the model-hole capacity opening as the test influencing factors. It showed that there was no approximative change trend in the influence of the rotational speed and the model-hole capacity opening on the seeding

rate. When only the rotational speed was used as the influencing factor to perform the one-variable linear fitting, the rotational speed had a significant effect on the seeding rate under different model-hole capacity openings ($R^2 > 0.99$). Therefore, this study used a linear regression analysis to obtain the theoretical value of the matching seeding rate under high-speed working conditions.

3.6. Effect of Vibration Frequency on Seeding Performance

As shown in Table 6, the influence of vibration frequency on the seed discharging performance of the hole-wheel-type wheat or oil seed discharging device When the rotation speed is 20–40 r/min, the opening capacity of wheat and rape in the mold hole is 10, 15, and 20 mm. When the capacity opening is 2, 3, and 4 mm, the variation coefficient of rate stability corresponding to each opening is not more than 3%. It is concluded that the vibration frequency has no significant effect on the rate of the hole-wheel-type row, which proves that the row is in the range of 0–10 Hz vibration frequency. The seed device has better performance and can be used in different vibration environments.

Table 6. Influence of vibration frequency on seed metering device performance of model-hole-wheel for both wheat and rapeseed.

Type of Seed	Working Rotational Speed r/min	Model-Hole Capacity Opening mm	Vibration Frequency 0 Hz 0 Hz in a Single Simulation	Vibration Frequency 5 Hz	Vibration Frequency 10 Hz	*C*v1 /%
			mv/(g·min^{-1})	mv/(g·min^{-1})	mv/(g·min^{-1})	
Shengyou 664	20	2	3.89	3.75	3.66	2.51%
		3	5.66	5.59	5.90	2.32%
		4	8.32	8.20	8.78	2.96%
	30	2	5.17	4.99	4.81	2.95%
		3	8.38	8.11	8.08	1.64%
		4	12.12	12.55	12.41	1.45%
	40	2	6.65	6.53	6.23	2.73%
		3	10.44	10.34	10.23	0.83%
		4	16.43	16.35	16.29	0.35%
Xuke No. 1	20	10	41.43	40.16	39.94	1.62%
		15	60.26	60.94	59.47	1.00%
		20	84.93	81.52	80.50	2.30%
	30	10	59.06	58.04	57.38	1.19%
		15	87.13	88.71	84.03	2.24%
		20	118.18	116.73	112.46	2.10%
	40	10	76.85	76.84	74.34	1.55%
		15	113.85	118.06	112.54	2.05%
		20	159.71	155.04	151.42	2.18%

4. Conclusions

The results showed that the average seeding rate of the inverted-fin-shaped model-hole-wheel was higher than the other three types of model-holes, and under different vibration frequencies, the variation coefficients of seeding rate stability were all less than 4%. The rotational speed significantly affected the seeding rate, while the vibration frequency had no significant effect on the seed filling process, and the seeding rate stability coefficients of variation were all less than 5%, indicating that the inverted-fin-shape of the model-hole-wheel has strong seed metering adaptability and stability, and the model has a certain universality.

The reasons for the better seed filling effect of the inverted-fin-shaped model-hole were discovered. According to the working characteristics of the model-hole-wheel, the seed filling room was divided into the actual seed filling area and the drag seed filling area

according to the population speed. In the simulation test, the number of seeds filled with inverted-fin-shaped holes was the most stable, and due to the perturbation effect of the small radius arc on the population, the population speed in the actual seed filling area was higher, and the disturbance effect was better, which was helpful for the model-hole filling. In the drag filling area, the contact between the population and the model-hole-wheel was dragged, and the relative speed of the population and the model-hole-wheel was reduced, which further improved the seed filling efficiency of the model-hole-wheel. The inverted-fin-shaped model-hole-wheel was verified by the bench test, and the results proved that the model-hole can meet the wheat agronomic requirements for sowing.

Author Contributions: Conceptualization, Z.L.; methodology, J.Z.; software, H.Z.; validation, W.W.; formal analysis, X.G.; investigation, X.G.; resources, L.C.; data curation, T.Z.; writing—original draft preparation, J.Z.; writing—review and editing, Z.L.; supervision, Z.L.; project administration, Y.C. All authors have read and agreed to the published version of the manuscript.

Funding: The authors gratefully appreciate the financial support provided by the National Natural Science Foundation of China (Grant No. 51805004), the Natural Science Foundation Project of Anhui Province (Grant No. 2008085QE217), and the Cooperative Research Project of universities in Anhui Province: Research on Unmanned Equipment in tillage and sowing Operations for Smart Agriculture (NO: GXXT-2020-011).

Institutional Review Board Statement: Not applicable.

Informed Consent Statement: Not applicable.

Data Availability Statement: The data presented in this study are available on request from the corresponding author.

Conflicts of Interest: The authors declare no conflict of interest.

References

1. Li, X.R.; Zhang, Y.P.; Diao, P.S.; Wang, Z.W.; Yao, W.Y.; Wang, Z.B. General Situation of Vegetable Production and Research Status of Precision Seeder in China. *Res. Agric. Mech.* **2021**, *43*, 263–268.
2. Boydas, M.G.; Tugut, N. Effects of vibration, roller design, and seed rates on the seedflow evenness of studded feed roller. *Appl. Eng. Agric.* **2007**, *23*, 413–418. [CrossRef]
3. Maleki, M.R.; Jafari, J.F.; Raufat, M.H.; Mouazen, A.M.; De Baerdemaeker, J. Evaluation of Seed Distribution Uniformity of a Multi-flight Auger as a Grain Drill Metering Device. *Biosyst. Eng.* **2006**, *94*, 535–543. [CrossRef]
4. Zagainov, N.; Kostyuchenkov, N.; Gao, X.J.; Li, Q.W.; Mi, G.P.; Huang, Y.X. Design and testing of novel seed miss prevention system for single seed precision metering devices. *Comput. Electron. Agric.* **2022**, *198*, 107048.
5. Luo, X.W.; Liu, T.; Jiang, E.C.; Li, Q. Design and experiment of direct seeding wheel for rice precision measuring model-hole. *Trans. Chin. Soc. Agric. Eng.* **2007**, *23*, 108–112.
6. Zhao, X.; Yu, H.; Zhang, J.; Huo, X.; Chen, F.; Zhao, J. Slot-type Pneumatic Precise Wheat Seed-metering Device. *J. Agric. Mach.* **2013**, *44*, 48–51.
7. Pareek, C.M.; Tewari, V.K.; Machavaram, R.; Nare, B. Optimizing the seed-cell filling performance of an inclined plate seed metering device using integrated ANN-PSO approach. *Artif. Intell. Agric.* **2021**, *5*, 1–12. [CrossRef]
8. Zhang, S.; Xia, J.; Zhou, Y.; Zhai, J.; Guo, Y.; Zhang, X.; Wu, H. Design and experiment of pneumatic cylinder-type precision direct seed-metering device for rice. *Trans. Chin. Soc. Agric. Eng.* **2015**, *31*, 11–19.
9. Li, Z.D.; Wang, Q.Q.; Zhang, Y.L.; Wang, W.W.; Yang, Y.L.; Chen, L.Q. Design and Experiment of Inclined Parabolic Cell Wheel in Seed Feeding Device for Wheat. *Trans. Chin. Soc. Agric. Mach.* **2018**, *9*, 116–124.
10. Panning, J.W.; Kocher, M.F.; Smith, J.A.; Kachman, S.D. Laboratory and field testing of seed spacing uiformity for sugarbeet planters. *Appl. Eng. Agric.* **2000**, *16*, 7–13. [CrossRef]
11. Liu, C.L.; Wei, D.; Du, X.; Jiang, M.; Song, J.N.; Zhang, F.Y. Design and Test of Wide Seedling Strip Wheat Precision Hook-hole Type Seed-metering Device. *Trans. Chin. Soc. Agric. Mach.* **2019**, *50*, 75–84.
12. Gao, X.J.; Cui, T.; Zhou, Z.Y.; Yu, Y.B.; Xu, Y.; Zhang, D.X.; Song, W. DEM study of particle motion in novel high-speed seed metering device. *Adv. Powder Technol.* **2021**, *32*, 1438–1449. [CrossRef]
13. Jin, M.F.; Ding, Y.Q.; Yu, H.F.; Liu, H.T.; Jiang, Y.Z.; Fu, X.Q. Optimal Structure Design and Performance Tests of Seed metering Device with Fluted Rollers for Precision Wheat Seeding Machine. *IFAC-PapersOnLine* **2018**, *51*, 509–514.
14. Lai, Q.H.; Jia, G.X.; Su, W.; Hong, F.W.; Zhao, J.W. Design and Test of Ginseng Precision Special-hole Type Seed-Metering Device with Convex Hull. *J. Agric. Mach.* **2020**, *51*, 60–71.

15. Lei, X.L.; Hu, H.J.; Wu, W.C.; Liu, H.N.; Liu, L.Y.; Yang, W.H.; Zhou, Z.L.; Ren, W.J. Seed motion characteristics and seeding performance of a centralised seed metering system for rapeseed investigated by DEM simulation and bench testing. *Biosyst. Eng.* **2021**, *203*, 22–33. [CrossRef]
16. Zhang, T.; Zhang, W.Z.; Chen, Z.W.; Wang, X.H.; Xu, Y.; Cui, X.J. Simulation Research on Seed Filling Performance of Spoon-belt Potato Seed Metering Device Based on EDEM. *Jiangsu Agric. Sci.* **2021**, *49*, 181–185.
17. Woo, S.M.; Uyeh, D.D.; Sagong, M.S.; Ha, Y.S. Development of seeder for mixed planting of corn and soybeans. *Int. J. Agric. Biol. Eng.* **2017**, *10*, 95–101.
18. Li, Z.D.; Yang, W.C.; Zhang, T.; Wang, W.W.; Zhang, S.; Chen, L.Q. Design and suction performance test of sucking-seed plate combined with groove-tooth structure on high speed precision metering device of rapeseed. *Trans. Chin. Soc. Agric. Eng.* **2019**, *35*, 12–22.
19. Ding, L.; Yang, L.; Liu, S.R.; Yan, B.X.; He, X.T.; Zhang, D.X. Design of air suction high speed precision maize seed metering device with assistant seed filling plate. *Trans. Chin. Soc. Agric. Eng.* **2018**, *34*, 1–11.
20. Shi, S.; Zhang, D.X.; Yang, L.; Cui, T.; Li, K.H.; Yin, X.W. Simulation and verification of seed-filling performance of pneumatic-combined holes maize precision seed-metering device based on EDEM. *Trans. Chin. Soc. Agric. Eng.* **2015**, *31*, 62–69.
21. Li, Z.D.; He, S.; Zhong, J.Y.; Han, J.F.; Chen, Y.X.; Song, Y. Parameter optimization and experiment of the disturbance pneumatic plate hole metering device for rapeseed. *Chin. J. Agric. Eng.* **2021**, *37*, 1–11.
22. Wang, Q.; Zhu, L.T.; Li, M.W.; Huang, D.Y.; Jia, H.L.; Zhuang, J. Vibration characteristics of com no-tillage finger-type precision planter and its effect on seeding performance. *Trans. Chin. Soc. Agric. Eng.* **2019**, *35*, 9–18.
23. Jiang, Y.J.; Liao, Y.T.; Qin, C.; Guan, Z.H.; Liao, Q.X. Vibration analysis and improvement for frame of 4SY-2.9 typed rape windrower. *Trans. Chin. Soc. Agric. Eng.* **2017**, *33*, 53–60.
24. Liu, H.; Zhou, J.L.; Zhang, R.F.; Shi, S.; Wei, G.J. Design and Test of Rotary Tilling Ridger of Puerarialobata. *Agric. Mech. Res.* **2021**, *43*, 158–163.
25. Li, Z.; Liao, Y.; Zhang, W.; Liao, Q. EDEM-based numerical simulation and analysis on filling performance of centralized seed metering device. *Int. Agric. Eng. J.* **2017**, *4*, 140–148.

Disclaimer/Publisher's Note: The statements, opinions and data contained in all publications are solely those of the individual author(s) and contributor(s) and not of MDPI and/or the editor(s). MDPI and/or the editor(s) disclaim responsibility for any injury to people or property resulting from any ideas, methods, instructions or products referred to in the content.